

Improved Analysis of EGMS Data for Displacement Monitoring: The Case Study of Regina Montis Regalis Basilica in Vicoforte, Italy

Davide Lodigiani^a, Marica Franzini^b and Vittorio Casella^c

Department of Civil Engineering and Architecture, University of Pavia, Via Ferrata 3, Pavia, Italy

Keywords: Cultural Heritage Conservation, SAR, Persistent Scatterers, Deformation Monitoring, Time Series.


Abstract: The Basilica of Vicoforte has always interested geotechnical engineers due to its location in a geologically complex area. One part of the Basilica is built on marl, while the other is built on clay. These two types of soil have different mechanical properties, which have caused the Basilica to experience various foundation failures over time. Monitoring is necessary to evaluate structural evolution and prevent further damage. Radar images are one of the geomatics techniques that can be used to perform these types of analyses; however, SAR data processing is challenging and requires specialized skills and software to monitor deformations using the PSInSAR approach. The European Ground Motion Service (EGMS) is useful for users and researchers, but analyzing specific buildings or monuments requires a more refined grid. The paper proposes a package of codes implemented using MATLAB release 2023b to manage grid spacing flexibly, customize it according to structure dimensions, and manage potential blunders. After a thorough data analysis, it was concluded that the monument exhibits no signs of subsidence trends. Instead, the analysis revealed that it undergoes seasonal fluctuations closely associated with temperature changes. The proposed approach enhances data accuracy and reliability, resulting in valuable insights and informed decisions.


1 INTRODUCTION


Italy is a country that boasts a diverse and extensive cultural heritage, which has made it a popular tourist destination for decades. The country's cultural treasures are spread across its diverse regions and span several millennia of human history. Artistically, Italy is home to some of the world's most famous artworks, from the masterpieces of the Renaissance to contemporary art. The country's archaeological heritage is equally impressive, with ancient ruins and monuments scattered throughout its countryside.

According to UNESCO estimates, Italy is home to a significant portion of Europe's cultural heritage, including artistic, archaeological, architectural, and environmental treasures (Benedikter, 2004). Since its establishment, UNESCO has organized and facilitated several conferences and conventions that focus on conserving and restoring cultural artifacts, historical sites, and traditions significant to humanity's shared history and knowledge (Accardo et

al., 2003). The Italian Government has actively promoted and founded various projects to provide tools for preserving cultural heritage and mitigating risks. Some of these projects are focused on raising awareness about the importance of damage prevention and reducing or eliminating its causes. Geological hazards such as soil movements, landslides, flooding, earthquakes, vulcanism, sinkholes, cavities, and subsidence are among these causes and pose significant risks to preserving Italian cultural heritage. The Geo-Risks Assessment and Mitigation for the Protection of Cultural Heritage (GIANO) project is an Italian initiative that focuses on assessing and mitigating geohazards that risk the country's cultural heritage. The project has two main objectives. Firstly, it aims to develop a robust protocol for accurately quantifying the risks posed by geohazards to Italy's cultural heritage. Secondly, it aims to identify the most effective and least invasive geotechnical mitigation techniques that can be used

^a  <https://orcid.org/0009-0009-5082-2022>

^b  <https://orcid.org/0000-0002-3921-5178>

^c  <https://orcid.org/0000-0003-2086-7931>

for different monumental constructions to address these hazards.

The GIANO project examines 14 noteworthy combinations of historical landmarks and geohazards. The list includes famous archaeological sites like the Etruscan necropolis of Tarquinia and Pompeii, churches such as Santa Maria Maggiore in Maratea and San Paolo Cathedral in Rome, and castles like Calatabiano and San Felice in Panaro. Among these sites, and the subject of this paper, is the Basilica of Regina Montis Regalis in Vicoforte. In particular, this church is facing a geological hazard due to uneven foundation settling caused by non-uniform deposits.

Unfortunately, the involved structures often lack the monitoring systems that are helpful for the GIANO project, resulting in insufficient data to assess the structural conditions and any deformations over time. This also makes it challenging to determine the history of past deformations that the structure has undergone. Consequently, conducting reliable numerical and risk scenario modeling becomes impossible, reducing the ability to protect and prevent these monuments from the effects of natural hazards. Despite having some structural information, the Basilica of Vicoforte lacks a historical terrain deformation dataset.

Geomatics has several effective non-invasive monitoring systems for identifying and tracking geohazards associated with ground movement or slope instability affecting cultural heritage structures. Deformation monitoring can be accomplished using techniques like high-precision GNSS, spirit leveling, high-precision topographic surveying, and satellite-based SAR (Synthetic Aperture Radar) interferometry. Differential Interferometric Synthetic Aperture Radar (DInSAR) is a sophisticated type of radar technology that employs multiple Synthetic Aperture Radar (SAR) images to detect and measure even the slightest changes in the Earth's surface over time (Blanco-Sánchez et al., 2008). The technique compares SAR images acquired at different times and uses the data to generate precise ground deformation maps. This remote sensing technique is especially valuable for detecting and monitoring surface deformation in areas with geological hazards, such as landslides (Cascini et al., 2010), volcanic activities (Hooper et al., 2004), and earthquakes (Wright et al., 2004). By allowing scientists to detect and monitor subtle ground movements, DInSAR plays a crucial role in understanding and predicting geological phenomena and ensuring the safety of people and infrastructure in vulnerable areas (Crosetto et al., 2016).

Persistent Scatterers InSAR (PSInSAR) falls under the differential interferometric Synthetic Aperture Radar (SAR) group. This technique uses stable reflective points with strong radar signal reflectivity and maintains temporal stability over time (Ferretti et al., 2001). Exploiting the permanent properties of scatterers, atmospheric effects can be filtered out, and geometrical decorrelation can be eliminated. Numerous missions, such as the C-band ERS mission and the more recent X-band SAR missions, COSMO-SkyMed and TerraSAR-X, have been developed over the years. These missions have enabled the systematic acquisition of thousands of interferometric data stacks worldwide, allowing for the precise measurement of surface deformations at a high spatial resolution and with millimetric-level precision. Best of all, it is a cost-effective alternative to traditional geodetic observations and does not require any ground-based instruments to be installed. The historical archive of more than 30 years allows the reconstruction of past deformations and the analysis of their evolution over time.

The Copernicus programme (Jutz & Milagro-Pérez, 2020; Showstack, 2014) is a crucial aspect of this framework and deserves special attention. The project involves two radar sensors, the Sentinel-1A and 1B (S1A and S1B), designed to collect interferometric C-band Synthetic Aperture Radar (SAR) image stacks on a global scale. These sensors are equipped to monitor ground deformation over Earth's surface accurately. The temporal resolution of the mission is impressive, with SAR image stacks collected every 6 days, allowing for precise monitoring of any changes that occur over time. Furthermore, the spatial resolution is equally impressive, with a resolution of about 10 meters. This level of accuracy enables us to obtain a detailed understanding of ground deformation processes occurring globally (Torres et al., 2020; Torres & Davidson, 2019).

SAR data is significant, leading to the development of a dedicated service within the Copernicus framework: the European Ground Motion Service (EGMS) (EMGS, 2024). The European Commission created this valuable tool to monitor and detect ground deformations using InSAR technology. The service processes and analyses all Sentinel-1 acquisitions over the Copernicus Participating States, providing a comprehensive and reliable platform for SAR data analysis and facilitating informed decision-making in various domains (Costantini et al., 2022).

The paper will describe the characteristics of the Basilica, focusing on monitoring the structures due to geotechnical issues. Specifically, displacement trends

could impact further stability, so it is important to conduct dedicated investigations. The EGMS will be utilized to achieve this, and its main features are described in Section 2. However, the online platform has an insufficient spatial resolution to perform reliable analysis, as discussed in Sections 2.1 and 2.2. To address this issue, Matlab codes and routines have been developed to manage grid spacing flexibly, customize it according to structure dimensions, and manage potential errors, as reported in Section 3. Finally, the results will be presented in Section 4, demonstrating that the Basilica does not suffer from any displacement trend but shows significant seasonal fluctuations closely associated with temperature changes.

1.1 The Regina Montis Regalis Basilica

The Regina Montis Regalis Basilica is a massive stone structure in Vicoforte, in northern Italy (Figure 1). This sanctuary is renowned for its extraordinary oval-shaped dome, which measures around 37x25 meters internally, making it the fourth-largest dome in the world (Chiorino et al., 2008).



Figure 1: View of the Regina Montis Regalis Basilica in Vicoforte.

Duke Charles Emmanuel I of Savoy originally envisioned the Basilica as the dynasty's mausoleum. The construction of this architecture commenced in 1596, with Ascanio Vittozzi (1583-1615) serving as the lead architect. Due to an unfortunate site selection, the building suffered from significant differential settlements in its foundations since the early stages of construction (Chiorino et al., 2008). The settlements were present due to the non-uniformity of the deposit. The site is characterized by a layer of compressible clayey silt that increases in depth from east to west. This layer rests on top of a marlstone layer that is exposed on the east side of the Basilica. Upon investigation, five of the Basilica's

eight pillars were found on the compressible soft layer. At the same time, the remaining three were placed directly on the marlstone (Bandera et al., 2023) due to this geological issue. However, concerns over the drum-dome system's structural safety emerged shortly after an extended system of asymmetric wide cracks opened (Figure 2).

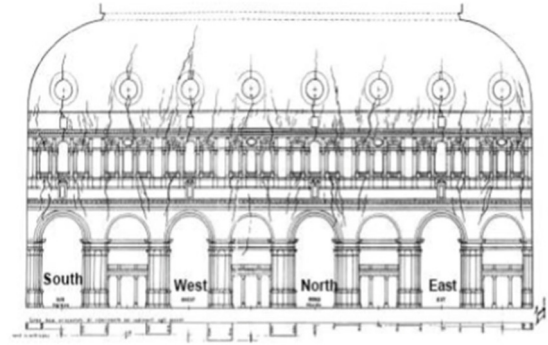


Figure 2: Pattern of the cracks observed by Eng. Garro on the Basilica of Vicoforte (Bandera et al., 2023).

The structural integrity of the Basilica has been monitored through permanent static (since 2004) and dynamic (since 2015) multi-sensor monitoring systems. The GIANO project aims to recreate settlements and study how the subsoil's stress-strain properties and behavior relate to the structure's behavior. An essential aspect of geotechnical numerical analyses is the geotechnical characterization of the site, which includes analyzing large-scale terrain deformations. This necessity forms the basis of using the PSInSAR technique for deformation monitoring.

2 THE EGMS SERVICE

EGMS is part of the Copernicus program, which involves 30 European states that process and analyze the Sentinel-1 dataset using a PSInSAR approach. The project has a monitoring timeframe from 2015 to 2021, with an annual update (European EnvironmentAgency (EEA), 2020).

The OpeRatlonal Ground motion INsar Alliance (ORIGINAL) consortium, spearheaded by e-GEOS from Italy, is responsible for data processing. The consortium also comprises TRE Altamira from Italy, NORCE from Norway, GAF AG from Germany, and the support of five other companies. The processing considers 750 S1 SAR SLC images, and each stack consists of 260 SAR scenes for the baseline product. The data utilized for processing requires a large

amount of disk space, approximately 1.5 PB, which is expected to increase by 350 TB annually (Crosetto et al., 2020, 2022).

As previously mentioned, this service is based on the Sentinel-1 constellation, which consists of two satellites: Sentinel-1A and Sentinel-1B. Sentinel-1A has operated since April 3, 2014, while its twin, Sentinel-1B, was launched into orbit on April 25, 2016. Both satellites have a C-band SAR sensor and use the Terrain Observation Progressive Scan SAR (TOPSAR) mode to acquire data (De Zan & Guarnieri, 2006). The Interferometric Wide Swath (IWS) satellite imaging mode is a feature that enables the sensor to capture high-resolution satellite images with exceptional detail and coverage. With this mode, the images can be obtained with a remarkable spatial resolution of 5 meters in the direction parallel to the satellite's line of flight (azimuth) and 20 meters along the range. Moreover, the acquired area is extensive, covering 200 kilometers along the azimuth and 250 kilometers along the range. This wide coverage provides a more comprehensive view of the area, making it ideal for large-scale mapping, land-use monitoring, and environmental studies. Additionally, this mode provides a revisit time of 12 days for a single satellite, which means that the same area can be imaged every 12 days. When two satellites are in orbit, the revisit time is reduced to only six days, allowing for more frequent and timely monitoring of the area (Torres et al., 2012). EGMS is a well-documented service reported in Costantini et al., 2021; Crosetto et al., 2020, 2021; Del Soldato et al., 2021).

The system offers a web-based interface that is available to all users. This interface allows users to search for a specific location and view a map of all scatterers detected in the selected area. By selecting a scatterer, the system generates a graph that displays its displacements over time. Noticeable, the platform is not limited to displaying time series; it allows registered users to download the raw data in the form of tables in three different ways (Crosetto et al., 2021):

1. Basic (Level L2A): basic units of measurement, which contain the displacement data along the satellite's line of sight as provided in the original radar geometry grid, with geolocation and quality indicators for each measurement point. These products are generated for each relative orbit of satellite image stacks;
2. Calibrated (Level L2B): these products are derived from Level 2A products and are aligned to a standard reference frame using external information such as GNSS data. The Level 2B

products are also integrated and mosaicked using best geodetic practices, and they are connected to the EUREF datum for consistency;

3. Ortho (Level 3): East-West and Up-Down deformation rates produced by combining Level 2B data from ascending and descending orbits, allowing the East-West and Up-Down components of the deformation rates to be estimated. The Level 3 products are resampled on a grid with 100 m x 100 m.

2.1 Data Visualization

On the EGMS platform, you can view points at different levels - L2A, L2B, or L3. The L2A and L2B levels only show movement along the line of sight, while the L3 level allows you to separate horizontal (East-West) and vertical (Up-Down) displacements. However, it is worth noting that the PSs are divided into 100x100 meter cells at the L3 level, which might not be appropriate for all applications. Besides, the grid is set by the platform and cannot be adapted to the different needs of the users.

This limitation becomes even more apparent when analyzing a structure's deformation or displacement, such as the Basilica of Vicoforte. In this scenario, the platform identifies the grid points near the church rather than directly on it. As a result, the displayed displacements are the outcome of averaging results originating from permanent scatterers located on the cathedral and its neighboring elements (Figure 3).

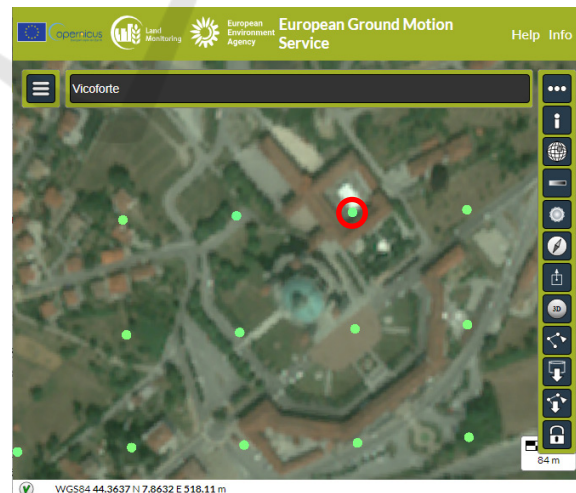


Figure 3: The 100x100-meter grid over the Basilica of Vicoforte available on the EGMS platform. The background is the VHR Image Mosaic 2018 (Copernicus, European Environment Agency).

Then, after selecting a location of interest, such as the red circle shown in Figure 3, a time series graph corresponding to that location is opened. The chart displays the date of each acquisition on the x-axis and the corresponding displacements in millimeters on the y-axis. The default setting shows the vertical displacements for the L3 level, but using the Data Selection Window, it is also possible to display the other information.

Figure 4 displays a visualization example, precisely the gridded point highlighted in Figure 3. This visualization illustrates horizontal and vertical displacement and includes a synthetic summary showing the annual mean velocity and the standard deviation. However, the 100 x 100-meter grid averaging process makes identifying any clear trend or seasonality difficult.

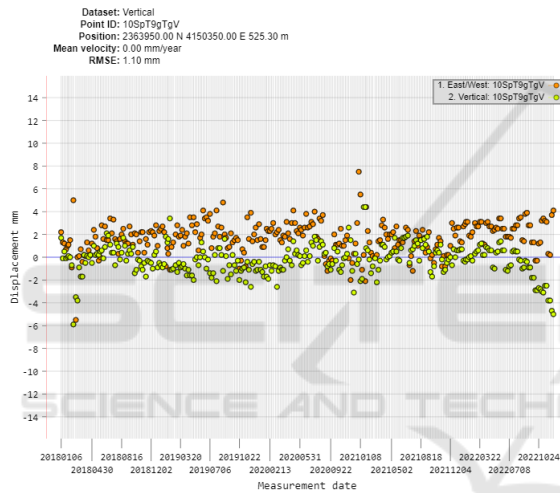


Figure 4: Example EGMS chart showing both horizontal and vertical displacement for a gridded point (L3 level).

2.2 Anomalous Data Management

It is crucial to remove any outliers from a dataset as they deviate significantly from the behavior of the rest of the data. In SAR data, outliers may arise from measurement errors, atmospheric errors, or surface changes. When considering displacement time series, removing anomalous or erroneous values is particularly important because they could significantly affect the interpretation of the outcomes. Rejecting blunders makes it possible to obtain a homogeneous and reliable time series.

Unfortunately, the EGMS platform does not allow the user to control the removal of outliers from the displacement time series. The user cannot select the most suitable method for rejecting data in their case study, nor can they assess the effect of outliers on the

results. This inflexibility limits the user's capacity to interpret the data accurately and draw sound conclusions.

Figure 4 depicts an example of this issue with some isolated points. Without proper knowledge and control of data processing, it is challenging to differentiate between blunders and actual values.

3 METHODOLOGY

Processing SAR datasets can be challenging, requiring specific skills and dedicated software packages. The PSInSAR approach is necessary to monitor deformations. Therefore, massive data must be processed to create the time series.

The EGMS service is a valuable tool for conducting this analysis, especially for newbies. The EGMS consortium extracts persistent scatterers (PS) for ascending and descending orbits and provides them on the web platform. This information is then combined at the L3 level to generate vertical and horizontal displacements in a gridded format. However, as mentioned in the conclusion of Section 2, the data provided may not be sufficient for analyzing a particular building or monument. In such instances, a more refined grid is necessary as a grid spacing of 100 meters is too coarse.

Within the GIANO project, the dome's behavior at the Regina Montis Regalis Basilica in Vicoforte requires careful analysis and a comparison to surrounding buildings; in this case, the EGMS platform's simple consultation is insufficient.

To address these limitations, a package of codes was implemented using MATLAB release 2023b. This approach has two main advantages: managing grid spacing flexibly and customized according to structure dimension and managing the presence of potential blunders. Implementing this approach makes enhancing the data's accuracy, consistency, and reliability feasible, resulting in more valuable insights and informed decisions.

3.1 EGMS Tables Management

The first step involves downloading the tables that contain L2B data for both ascending and descending geometry for a selected area. However, even if a region of interest (ROI) is given, the platform manages the data according to the burst of reference S1 image. Hence, the persistent scatterers downloaded refer to a larger area. This results in a significant amount of data, which, in our case, takes up around 1.5 GB per table.

A specific code enables the selection of persistent scatterers available inside the ROI, disregarding all others and speeding up the following steps.

3.2 Grid Generation and PSs Indexing

Once both tables have been reduced to the scatterers present in the ROI, they can be organized according to the analysis requirements.

The ROI usually has a square or rectangular shape, so it can be divided into a grid with regular spacing determined using a parametric approach. Each cell inside the ROI can be identified by an ID consisting of two values representing its row and column position. The program then checks the position of each PS concerning the generated grid and assigns the corresponding ID.

Users can then set the cell size according to specific requirements, such as structure dimensions. However, it is important to note that the number of PSs available significantly impacts component decomposition. At least one ascending and descending PS is required for this operation, with having more than one PS improving robustness. Therefore, the cell size should be calibrated while considering this requirement.

3.3 Time Series Generation

Displacement time series can then be generated after harmonizing the two tables and indexing the PSs based on the selected grid. The tool is made up of several functions that allow you to perform the following tasks:

- Removing cells that contain PSs having discrepancies in their velocity values;
- Identifying outliers in the displacement time series and recalculating them;
- Remove cells containing only one PS.
- Calculate the average displacement data for ascending and descending geometries and place them at the cell's centroid.
- Standardizing displacement dates between two acquisition geometries by generating time-related average data (weekly, monthly, quarterly, yearly).
- Generating a series of plots useful for data interpretation and analysis.

The code tests the congruency of velocities between PSs in each cell; the Copernicus consortium determines velocities and available within the downloaded datasets. Simply removing the PSs that present such anomalies might not be sufficient to address the issue of inconsistent velocities. Indeed,

several scatterers in such cells are often found to be significantly different from one another. Therefore, removing the entire cell altogether was decided, providing greater accuracy. To understand which areas have adequate cell numerosity for subsequent steps, the code generates two graphs (one for each acquisition geometry), in which valid cells are highlighted in green and rejected cells in red.

Besides, to perform a slant displacement decomposition in horizontal and vertical components, at least two PSs are necessary - one for ascendant and one for descendant geometry. If a cell contains only one PS, the operation cannot be performed, and also, in this case, the cell will be removed from the next step.

The displacement time series of every PS is then checked for possible outliers. Sometimes, the datasets that contain the slant displacements may have anomalous values due to atmospheric errors or surface changes. If these values are not managed correctly, they can negatively impact the time series analysis. Instead of removing these values and creating a gap in the dataset, the code replaces them with the mean value between the previous and following displacement. Also, in this case, the code generates a graphical output for better interpretation.

Once the outliers have been replaced with average values, the code calculates the mean and standard deviation of the slant displacement for the two acquisition geometries in every cell. This allows the measurement to be regularized into a gridded format; the calculated values are associated with each cell's centroid coordinates. A graphic plot is also available for this step.

Finally, the observations for the two geometries, ascending and descending, are not taken simultaneously but with a few days' difference between them. To overcome this issue, the code performs a time average between the dates, according to the user's chosen criteria: weekly, monthly, quarterly, or yearly. This creates a consistent timetable for both acquisition geometries, which helps decompose the displacement into vertical and horizontal components.

Figure 5 illustrates the workflow described, with blue shapes representing functions and red ones indicating graphical outputs.

3.4 Slant Displacement Decomposition

By considering the slant displacements of the ascending and descending geometry for each cell, it is possible to calculate both vertical (up-down) and horizontal (east-west) displacement components

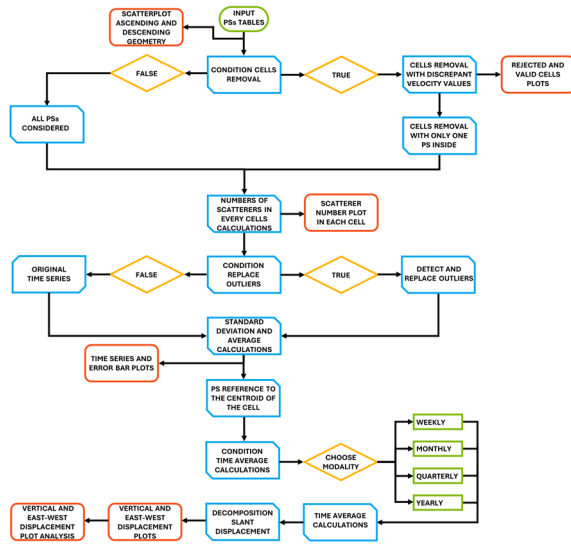


Figure 5: Workflow implemented in MATLAB environment.

(Fuhrmann & Garthwaite, 2019).

In particular, the two elements can be obtained:

$$\begin{bmatrix} d_{ver} \\ d_{hor} \end{bmatrix} = (A)^{-1} \begin{bmatrix} d_{asc}^{LOS} \\ d_{dsc}^{LOS} \end{bmatrix} \quad (1)$$

Matrix A has the following expression:

$$A = \begin{bmatrix} -\sin(\theta_{asc}) \cos(\alpha_{asc}) & \cos(\theta_{asc}) \\ -\sin(\theta_{dsc}) \cos(\alpha_{dsc}) & \cos(\theta_{dsc}) \end{bmatrix} \quad (2)$$

Variables have the following meanings:

- d_{ver} : vertical displacement (Up-Down);
- d_{hor} : horizontal displacement (East-West);
- d_{asc}^{LOS} : displacement along the satellite's line of sight in ascending geometry;
- d_{dsc}^{LOS} : displacement along the satellite's line of sight in descending geometry;
- θ_{asc} : angle of incidence of ascending geometry;
- θ_{dsc} : angle of incidence of descending geometry;
- α_{asc} : heading angle of ascending geometry;
- α_{dsc} : heading angle of descending geometry.

Understanding the displacement signs is crucial to comprehend the phenomenon in the selected area of interest. The vertical displacement is negative when it moves downwards away from the sensor, while it is positive when moving upwards towards the sensor. On the other hand, the horizontal displacement is positive when the point moves in the East direction, while it is negative when moving in the West direction. For a better understanding, please refer to Figure 6, which shows the legend of the signs for

vertical (Up-Down) and horizontal (East-West) displacements.

LEGEND DISPLACEMENT			
VERTICAL		HORIZONTAL	
DIRECTION	SIGN	DIRECTION	SIGN
↑ Upward	+	→ East	+
↓ Downward	-	← West	-

Figure 6: Legend vertical (Up) and planimetric (East-West) displacement.

4 RESULTS

The following is a selection of the results obtained for the area of Regina Montis Regalis Basilica in Vicoforte. The data used for the study spans five years, from February 2016 to December 2021. The section focuses on the immediate vicinity of the Basilica, which covers an area of 0.15 square kilometers, and focuses on a comprehensive analysis of the dome's behavior.

Figure 7 presents an orthophoto of the area with the persistent scatterers' availability displayed for both the ascending and descending geometries. These PSs are obtained from the L2B data collected from the EGMS platform and are used to determine vertical and horizontal displacements. The figure shows that some areas have scatterers derived from only one geometry, ascending or descending. The Basilica's dome has this behavior due to its structure configuration. Therefore, a careful choice of the grid size is necessary in this case.

Based on the previous sections, a smaller grid size is utilized to enhance the analysis of results obtainable using the standard L3 level. In the EGMS platform, a cell size of 100 m is used, whereas, concerning the dome dimension and PSs location, a cell size of 25 m is used here, which is a quarter of that. A total of 238 cells were created and distributed on 17 rows and 14 columns.

In order to gain a clearer understanding of the distribution of cells within the area of interest, a plot containing the grid and cell IDs is created. Figure 8 shows the generated grid, represented in black, superimposed onto the orthophoto of the area. Each cell containing at least one PS reports its index, represented by the number of rows and columns; empty cells correspond to areas without PS.

The code generates a figure displaying the grid with cell ID in black, the number of scatterers in

ascending geometry in red, and the number of scatterers in descending geometry in blue (Figure 9).

Figure 9 shows that many cells contain a quantity of PSs that are insufficient for performing the decomposition process. Therefore, cells with only ascending or descending scatterers and cells with velocity incongruent values must be discarded. Table 1 reports some statistical values on valid and rejected cells.

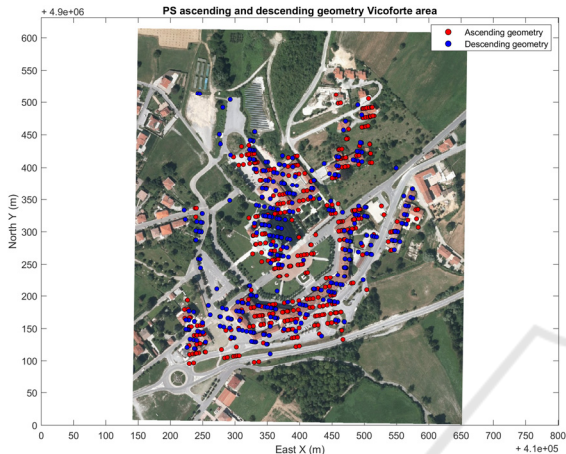


Figure 7: PSs positions for ascending acquisition geometry are in red, and the descending one is in blue. The background is the WMS service of the Piedmont region for the orthophoto AGEA 2018.



Figure 8: The grid created for the ROI has a cell size of 25 m. Each cell containing the PSs reports its index, represented by the number of rows and columns.

The EGMS platform partially bypasses the first issue, choosing to discretize the ground into cells of 100 m in size since there is more possibility of having ascending and descending PSs.

Fortunately, for GIANO project purposes, the cells containing the Basilica's Dome are sufficient in number and quality for the next steps. The cells involved are the (8,6) and (9,6).

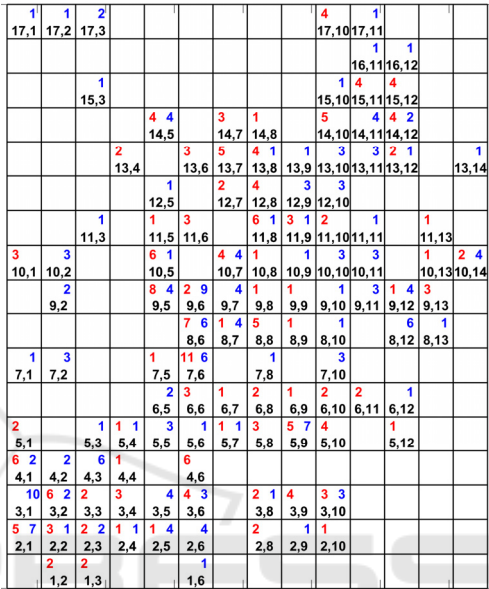


Figure 9: Each cell displays the ID in black, the number of ascending acquisition geometry scatterers in red, and the number of descending geometry scatterers in blue.

Table 1: Total number of valid and rejected cells.

Acquisition geometry	Total cells	Valid cells	Rejected cells
Ascending	108	71 (66%)	37 (34%)
Descending	107	73 (68%)	34 (32%)

4.1 Dome Displacements Analysis

Out of the two cells covering the dome, only the cell (8,6) will be considered as it has more PSs. This cell is located in the South-Western part of the Basilica's dome. Specifically, it consists of seven scatterers with ascending geometry and six with descending geometry.

The data was analyzed for outliers before performing slant displacement decomposition. Two figures were created to display the time series for ascending and descending geometry - Figure 10 and Figure 11, respectively. All present PSs (seven in the first figure and six in the second) were considered.

The code highlights any blunders found with a red point. Some values found blunders are relatively high for some PSs, especially for ascending geometry.

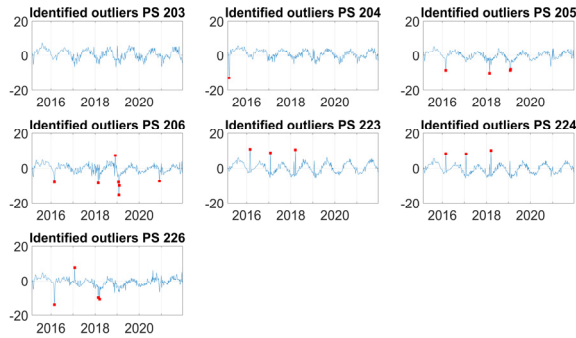


Figure 10: The outliers identified for the ascending geometry are indicated in red.

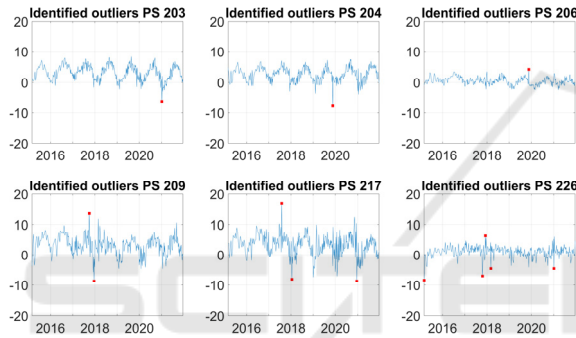


Figure 11: The outliers identified for the descending geometry are indicated in red.

After replacing the outliers with the mean displacement between the previous and following data points, the displacement values for all the PSs in the same cell are averaged and grouped by geometry. The plot in Figure 12 shows the time series for the slant displacement of the considered cell and the two geometries. The results for the ascending orbit are displayed in red, while those for the descending orbit are in blue. The vertical bars in a graph show the confidence interval of the mean, which is derived from the standard deviation. This allows us to visualize the spread of the data that contributed to the mean. The former geometry generally shows low standard deviation values, except for a few cases with high values.

Upon analyzing the time series data, it becomes immediately apparent that a recurring seasonal pattern is present over time. Instead, when analyzing the L3-level data present on the EGMS portal, this phenomenon is not readily discernible. This is because the L3-level data are aggregated at a coarser

level, masking the underlying seasonal pattern in the raw data.

Decomposing the displacement into its vertical and horizontal components is now possible. Figure 13 displays the displacement trend along with the associated confidence interval and confidence bounds. Both displacements exhibit a negligible annual displacement rate of -0.1 mm/year. Besides, the previously observed cyclic phenomenon depends mainly on vertical displacement. Focusing on 2020 and 2021, Figure 14 shows that the positive peaks occur in July-August, whereas the negative variation is probably due to the material used to construct the dome of the Basilica; indeed, it is made of copper, which tends to expand and contract based on the temperature, causing a change in its size. The horizontal displacement, on the other hand, seems to remain mostly stable.

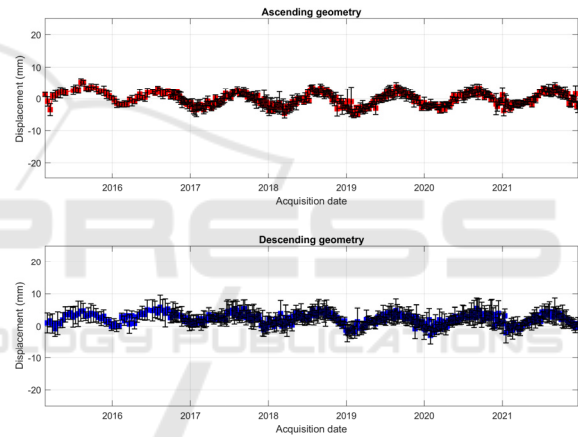


Figure 12: Slant displacement time series for the selected cell. Outcomes for ascending acquisition geometry are in red, whereas those for descending one are in blue.



Figure 13: Vertical and horizontal displacement time series for the selected cell.

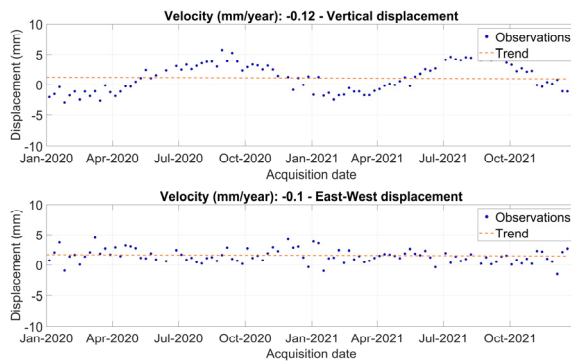


Figure 14: At the top is the vertical displacement time series, and at the bottom is the horizontal one. The time interval has been reduced to the last two years to show how the maximum peaks occur in the summer period (July-August) and the minimum peaks in the winter period (February-March).

The vertical and horizontal displacement signals were decomposed to understand the displacements better. This process allows the time series to be broken down into its components, which include the trend, seasonality, and residual. Figure 15 displays the vertical component of the displacement, where the trend indicates a drop in the structure's position by around 1.5 mm between 2015 and 2021. The seasonality is evident with a fluctuation of ± 2 mm, and the residual falls within the same range.

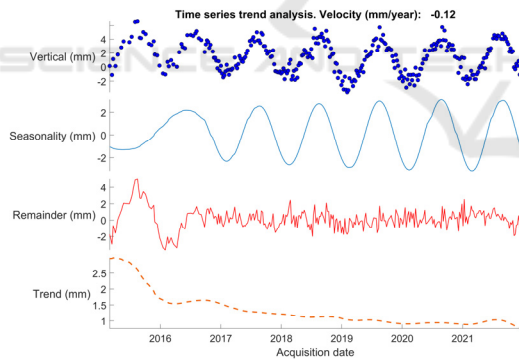


Figure 15: Decomposition of the vertical displacement time series for cell (8,6). From top to bottom, vertical displacement seasonality, remainder, and the time series trend.

Similarly, Figure 16 illustrates the horizontal displacement, which also shows a decreasing trend, although the displacement is only 0.6 mm over the considered period. From 2017 onwards, the contribution of seasonality appears to be much less pronounced than for the vertical component, with variations of ± 1 mm. Like the vertical shift, the residual seems to be within a range of ± 2 mm.

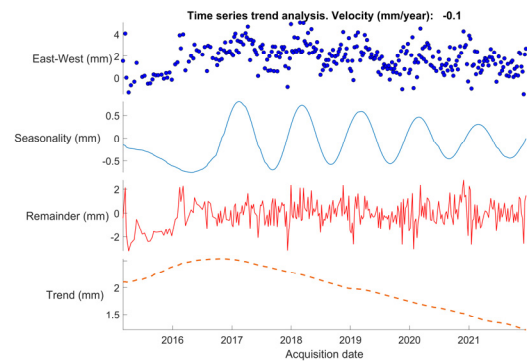


Figure 16: Decomposition of the horizontal displacement time series for cell (8,6). From top to bottom, vertical displacement seasonality, remainder, and the time series trend.

Based on the time series of displacement data, there are no significant deformations in the structure or the surrounding area. The deformations are negligible. No localized deformations were observed in the structure, but a seasonal pattern was identified in the vertical component. Specifically, a periodic signal was observed in the vertical displacement, with maximum peaks occurring in August and minimum peaks in January. Additionally, there is a slight seasonal component in the horizontal component, although it is not as significant as that of the vertical displacement.

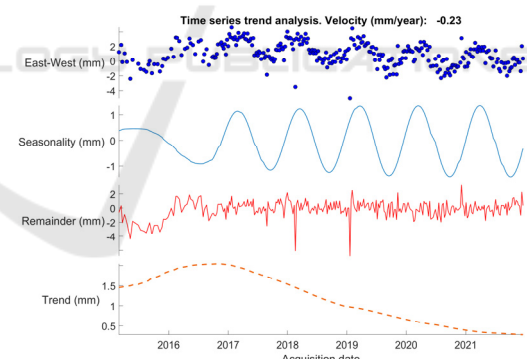


Figure 17: Decomposition of the vertical displacement time series for cell (9,6). From top to bottom, vertical displacement seasonality, remainder, and the time series trend.

It is worth noting that while cell (8,6) has the most significant number of PSs, it is possible to obtain similar information for other cells as well. For instance, Figure 17 shows the vertical displacement of another cell, cell (9,6), located in the Basilica dome. The two cells display similar trends regarding average speed of movement and periodicity. This similar behavior demonstrates that using tuned parameters for PS analysis can improve the

interpretation of the EGMS datasets. However, further investigation is needed for 2016, as there are some conflicting values in Figures 15, 16, and 17.

5 CONCLUSION

The Basilica of Vicoforte is a magnificent religious structure in a geologically complex area. It is even more fascinating because it is built on two distinct geological formations - marl and clay. These two types of soil have different mechanical properties, which have caused the Basilica to experience various foundation failures over time. These failures have resulted in cracks, detachments, and deformations in the dome and other structure parts. Due to these issues, the Basilica has required numerous restoration and consolidation works since its construction. As a result, geo-technicians continually monitor the Basilica to detect new subsidence and intervene promptly to ensure the structure's integrity.

Geomatics offers a range of noninvasive systems to monitor structural deformation and displacement. The Basilica has some monitoring systems, primarily consisting of accelerometers, which measure the frequency of structural movements. However, a means to measure deformation concerning an external stable framework was not available in the short or long term. Therefore, a radar approach was employed.

SAR data processing is a complex and challenging task that requires specialized skills and software. A more refined grid is necessary to monitor deformations using the PSInSAR approach, especially when analyzing specific buildings or monuments. While the EGMS service can be helpful for general purposes, it may not provide the necessary detail for analyzing specific structures. Fortunately, a package of codes implemented using MATLAB release 2023b can flexibly manage grid spacing, customized according to the dimensions of the structure under consideration. This approach offers greater control over the data, making it possible to identify and manage potential blunders. It also enhances data accuracy and reliability, providing valuable insights to inform decisions.

The analysis with a customized MATLAB code package helped refine the size of the interpolation grid, manage the presence of any outliers, and analyze the vertical and horizontal movements in terms of seasonality and trends. Due to the aggregation level present on the EGMS platform, this was not directly possible with the original L3 level. The analysis highlighted a seasonal phenomenon on the dome of

the Basilica, presumably due to the expansion of the metal linked to temperatures, having an extent of around two millimeters. However, no subsidence trend is evident, recording movements of only 0.1 mm per year.

As no other displacement monitoring systems are available, comparing the obtained results with other measurements is not feasible. Nonetheless, the paper's primary aim was to enhance the analysis of data extracted from the EGMS database, and this objective was achieved successfully. As part of the GIANO project scope, other monitored monuments will be tested with the same analysis approach, selecting those with additional monitoring sensors.

ACKNOWLEDGMENTS

The authors thank the Italian Ministry of University and Research (MUR) for funding the project through the PRIN 2020 scheme.

REFERENCES

- Accardo, G., Giani, E., & Giovagnoli, A. (2003). The risk map of Italian cultural heritage. *Journal of Architectural Conservation*, 9(2). <https://doi.org/10.1080/13556207.2003.10785342>
- Bandera, S., Giffirè, D., & Lai, C. G. (2023). Geotechnical Characterization of the Subsoil at the "Regina Montis Regalis" Basilica in Vicoforte, Italy. *Springer Series in Geomechanics and Geoengineering*. https://doi.org/10.1007/978-3-031-34761-0_59
- Benedikter, R. (2004). Privatisation of Italian cultural heritage. *International Journal of Heritage Studies*, 10(4). <https://doi.org/10.1080/1352725042000257393>
- Blanco-Sánchez, P., Mallorquí, J. J., Duque, S., & Monells, D. (2008). The coherent pixels technique (CPT): An advanced DInSAR technique for nonlinear deformation monitoring. *Pure and Applied Geophysics*, 165(6). <https://doi.org/10.1007/s00024-008-0352-6>
- Cascini, L., Fornaro, G., & Peduto, D. (2010). Advanced low- and full-resolution DInSAR map generation for slow-moving landslide analysis at different scales. *Engineering Geology*, 112(1–4). <https://doi.org/10.1016/j.enggeo.2010.01.003>
- Chiorino, M. A., Spadafora, A., Calderini, C., & Lagomarsino, S. (2008). Modeling strategies for the world's largest elliptical dome at Vicoforte. *International Journal of Architectural Heritage*, 2(3). <https://doi.org/10.1080/15583050802063618>
- Costantini, M., Minati, F., Trillo, F., Ferretti, A., Novali, F., Passera, E., Dehls, J., Larsen, Y., Marinkovic, P., Eineder, M., Brcic, R., Siegmund, R., Kotzerke, P., Probeck, M., Kenyeres, A., Proietti, S., Solari, L., & Andersen, H. S. (2021). EUROPEAN GROUND

- MOTION SERVICE (EGMS). *International Geoscience and Remote Sensing Symposium (IGARSS)*, 2021-July. <https://doi.org/10.1109/IGARSS47720.2021.9553562>
- Costantini, M., Minati, F., Trillo, F., Ferretti, A., Passera, E., Rucci, A., Dehls, J., Larsen, Y., Marinkovic, P., Eineder, M., Brcic, R., Siegmund, R., Kotzerke, P., Kenyeres, A., Proietti, S., Solari, L., & Andersen, H. (2022). EGMS: a New Copernicus Service for Ground Motion Mapping and Monitoring. *EGU General Assembly 2022*, 23-27 May 2022.
- Crosetto, M., Monserrat, O., Cuevas-González, M., Devanthery, N., & Crippa, B. (2016). Persistent Scatterer Interferometry: A review. In *ISPRS Journal of Photogrammetry and Remote Sensing* (Vol. 115). <https://doi.org/10.1016/j.isprsjprs.2015.10.011>
- Crosetto, M., Solari, L., Balasis-Levinsen, J., Bateson, L., Casagli, N., Frei, M., Oyen, A., Moldestad, D. A., & Mróz, M. (2021). Deformation monitoring at european scale: The copernicus ground motion service. *International Archives of the Photogrammetry, Remote Sensing and Spatial Information Sciences - ISPRS Archives*, 43(B3-2021). <https://doi.org/10.5194/isprs-archives-XLIII-B3-2021-141-2021>
- Crosetto, M., Solari, L., Barra, A., Monserrat, O., Cuevas-González, M., Palamà, R., Wassie, Y., Shahbazi, S., Mirmazloumi, S. M., Crippa, B., & Mróz, M. (2022). ANALYSIS OF THE PRODUCTS OF THE COPERNICUS GROUND MOTION SERVICE. *International Archives of the Photogrammetry, Remote Sensing and Spatial Information Sciences - ISPRS Archives*, 43(B3-2022). <https://doi.org/10.5194/isprs-archives-XLIII-B3-2022-257-2022>
- Crosetto, M., Solari, L., Mróz, M., Balasis-Levinsen, J., Casagli, N., Frei, M., Oyen, A., Moldestad, D. A., Bateson, L., Guerrieri, L., Commerci, V., & Andersen, H. S. (2020). The evolution of wide-area DInSAR: From regional and national services to the European ground motion service. In *Remote Sensing* (Vol. 12, Issue 12). <https://doi.org/10.3390/RS12122043>
- De Zan, F., & Guarnieri, A. M. (2006). TOPSAR: Terrain observation by progressive scans. *IEEE Transactions on Geoscience and Remote Sensing*, 44(9). <https://doi.org/10.1109/TGRS.2006.873853>
- Del Soldato, M., Confuorto, P., Bianchini, S., Sbarra, P., & Casagli, N. (2021). Review of works combining GNSS and insar in Europe. In *Remote Sensing* (Vol. 13, Issue 9). <https://doi.org/10.3390/rs13091684>
- EMGS. (2024). EGMS. <https://egms.land.copernicus.eu/>
- European Environment Agency (EEA). (2020). Copernicus Land Monitoring Service 2020. *European Environment Agency (EEA)*.
- Ferretti, A., Prati, C., & Rocca, F. (2001). Permanent scatterers in SAR interferometry. *IEEE Transactions on Geoscience and Remote Sensing*, 39(1). <https://doi.org/10.1109/36.898661>
- Fuhrmann, T., & Garthwaite, M. C. (2019). Resolving three-dimensional surface motion with InSAR: Constraints from multi-geometry data fusion. *Remote Sensing*, 11(3). <https://doi.org/10.3390/rs11030241>
- Hooper, A., Zebker, H., Segall, P., & Kampes, B. (2004). A new method for measuring deformation on volcanoes and other natural terrains using InSAR persistent scatterers. *Geophysical Research Letters*, 31(23). <https://doi.org/10.1029/2004GL021737>
- Jutz, S., & Milagro-Pérez, M. P. (2020). Copernicus: The European earth observation programme. *Revista de Teledeteccion*, 2020(56). <https://doi.org/10.4995/raet.2020.14346>
- Showstack, R. (2014). Sentinel Satellites Initiate New Era in Earth Observation. *Eos, Transactions American Geophysical Union*, 95(26). <https://doi.org/10.1002/2014eo260003>
- Torres, R., & Davidson, M. (2019). Overview of Copernicus SAR Space Component and its Evolution. *International Geoscience and Remote Sensing Symposium (IGARSS)*. <https://doi.org/10.1109/IGARSS.2019.8899134>
- Torres, R., Davidson, M., & Geudtner, D. (2020). Copernicus Sentinel Mission at C- and L-Band: Current Status and Future Perspectives. *International Geoscience and Remote Sensing Symposium (IGARSS)*. <https://doi.org/10.1109/IGARSS39084.2020.9323149>
- Torres, R., Snoeij, P., Davidson, M., Bibby, D., & Lokas, S. (2012). The Sentinel-1 mission and its application capabilities. *International Geoscience and Remote Sensing Symposium (IGARSS)*. <https://doi.org/10.1109/IGARSS.2012.6351196>
- Wright, T. J., Parsons, B. E., & Lu, Z. (2004). Toward mapping surface deformation in three dimensions using InSAR. *Geophysical Research Letters*, 31(1). <https://doi.org/10.1029/2003GL018827>